

Pb–Ag Alloy Anode Modified with Polyaniline Film and its Electrochemical Performance in Sulfuric Acid Electrolyte

PeiPei Li¹, RenChun Fu^{*1}, Du Jun², Hui Huang^{2,3}, ZhongCheng Guo^{2,3}

¹ Department of science, Kunming University of Science and Technology, Kunming 650093, China;

² Department of Metallurgy and Energy Engineering, Kunming University of Science and Technology, Kunming 650093, China;

³ Kun Ming Hendera of Science and Technology Co.,Ltd.,Kunming 650106, China.

*E-mail: polymerminer@163.com

Received: 28 January 2019 / Accepted: 29 March 2019 / Published: 10 June 2019

The nature of the electrode surface plays an important role in the electrode reaction. In this study, Pb–Ag alloy anodes modified with polyaniline films were prepared by galvanostatic polymerisation. Linear scanning voltammetry (LSV), cyclic voltammetry and potentiodynamic polarisation were measured and compared with those of unprepared Pb–Ag (0.3 wt%) alloy anodes. The oxygen evolution reaction potential of the modified anodes was lower than that of the unprepared Pb–Ag (0.3 wt%) anode at same anodic current density. The corrosion resistance of the modified anode was better than that of the unprepared Pb–Ag (0.3 wt%) anode. SEM images were obtained to characterise the morphology of the polyaniline film, and FTIR spectra confirmed that the film coating the Pb–Ag alloy was polyaniline.

Keywords: polyaniline; cyclic voltammetry; linear scanning voltammetry; Pb–Ag alloy

1. INTRODUCTION

Pb–Ag (0.3–1 wt%) alloy is widely used as anode material for electrowinning of nonferrous metals, such as Cu, Zn, Ni, Co and Mn, because of its excellent corrosion resistance in acidic sulfate solution. However, Pb–Ag alloy anodes have high over potential of the oxygen evolution reaction (OER) and cause contamination of the Pb ion in the cathodic products. In the last decade, various methods have been developed to reduce the over potential of OER and prevent the dissolution of the Pb–Ag anodes. For example, Ca, Sn, Sr, Co, Sb, In, and Mn ions were dispersed in Pb–Ag alloys to make binary and ternary alloys [1 – 3]; noble metal oxides (RuO₂, IrO₂ and ZrO₂) [4,5] and base metal oxides (MnO₂, PbO₂, TiO₂, Co₃O₄ and SnO₂) [6–8] were used to coat Pb–Ag alloys to make dimensionally stable anode (DSA). Conductive polymer represents another approach to reduce the energy consumption of electrowinning and achieve pure cathodic products [9].

As one of the most frequently investigated conductive polymers, polyaniline (PANI) has been widely investigated, particularly its synthesis, structure and fundamental properties, such as conductivity, optical nonlinearity and mechanical performance [10 – 12]. Previous works indicated that conductive PANI is promising for many future practical applications. For example, conductive PANI was used as an electrode component to improve the electrocatalytic performance of the anode [13 – 15]; PANI and its composites were also used for protection of substrate metals [16, 17]. Researchers extensively studied the electrochemical syntheses of conductive PANI coatings on oxidisable metals for protection purposes. For example, the stability of the PANI film was improved [18], the protection mechanism was investigated [19, 20], and the electrocatalytic properties were improved [21]. Aniline electropolymerisation proceeds according to the following Figure 1 [22, 23]:

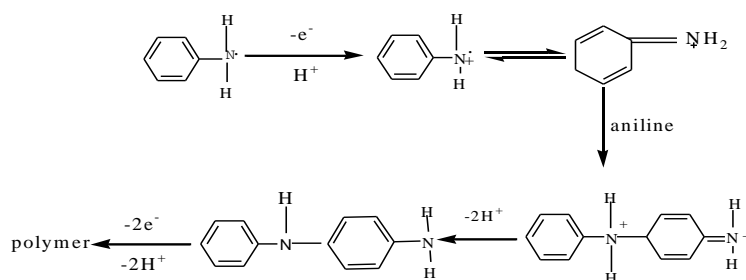


Figure 1. Mechanism of aniline electropolymerisation

Liao [24] demonstrated that Figure 1 was the mechanism of not only electro synthesised PANI film but also autocatalytic polymerized PANI film. The polymerisation process of electropolymerised PANI film on the metal substrate surface includes three stages [25].

For the electrowinning of nonferrous metals, the anode should reduce the OER potential and improve corrosion resistance. Therefore, this paper aims to prepare a PANI film on the surface of a Pb–Ag alloy anode and investigate the potential of OER and corrosion resistance of the modified anode. PANI films were prepared by galvanostatic polymerisation at different current densities. Potentiodynamic polarisation curves, scanning electron microscopy (SEM) images, cyclic voltammograms, X-ray photoelectron spectroscopy (XPS) spectra and LSV were employed to character the properties of the new anode.

2. EXPERIMENTS AND DETAILS

2.1 Chemicals and equipment

The chemicals used in this experiment were of analytical grade. Sulfuric acid (H₂SO₄) and aniline were purchased from Aladdin Chemistry Co., Ltd. The aniline was distilled under reduced pressure prior to use. Pb–Ag (0.3 wt%) alloys were purchased from Kunming Hendera Science and Technology Co., Ltd., China. Deionised water was used in all experiments. The electrochemical workstation was model CHI1760 made by Shanghai Chen Hua Co., Ltd.

2.2 Cleaning of the working electrode

Pb–Ag (0.3 wt%) alloy was cut into a 1 cm×1 cm×0.2 cm slide and polished by 400#, 800#, 1000#, and 1200# sand paper to obtain a mirror-bright surface and reduce the influence of the surface roughness. One side and four edges of the slide were cast with denture base resin (type II, Dental Materials Factory of Shanghai Medical Instruments Co. Ltd., China) with a working area of 1.0 cm². The working electrode was used immediately after it was sequentially rinsed with deionized water and acetone and dried at 50°C.

2.3 Electro polymerisation

The PANI film was electropolymerised in an aqueous solution containing aniline (0.2 mol L⁻¹) and H₂SO₄ (0.5 mol L⁻¹). The PANI modified anode was obtained by galvanostatic polymerisation at current densities of 0.5, 1.5, 2.5, 3.5 and 4.5 mA cm⁻² and time of 1200 s. Thus, five different PANI-modified anode samples were prepared. Galvanostatic polymerisation was carried out at 0.5 mA cm⁻² on Pb–Ag (0.3 wt%) alloy named PFPbAg-0.5. The 1.5 mA cm⁻² sample was named PFPbAg-1.5. The 2.5 mA cm⁻² sample was named PFPbAg-2.5. The 3.5 mA cm⁻² sample was named PFPbAg-3.5. The 4.5 mA cm⁻² sample was named PFPbAg-4.5.

2.4 Characterisation tests

Characterization tests were carried out after the PANI film on the Pb–Ag (0.3 wt%) alloy was rinsed with deionized water to remove any residual electrolyte and oligomers.

The electrochemical experiments (linear scanning voltammetry, cyclic voltammetry and potentiodynamic polarisation) were carried out in a three-electrode system. A saturated calomel electrode (SCE) was used as the reference electrode, and a platinum plate (2.5 cm²) was used as the counter electrode. The working electrodes were the unprepared Pb–Ag (0.3 wt%) alloy or PANI-modified anodes with geometric area of 1 cm² and thickness of 2 mm. During electrochemical experiments, the solution was not stirred, not deaerated or aerated, but simply exposed to air at room temperature.

The linear scanning voltammetry measurements were done at a scanning rate of 1 mV/s in 0.5 mol L⁻¹ H₂SO₄ aqueous solution.

The scan rate of cyclic voltammetry was 10 mV/s in 0.5 mol L⁻¹ H₂SO₄ and 0.2 mol L⁻¹ aniline.

At a constant scan rate of 1 mV·s⁻¹, potentiodynamic polarisation curves for the PANI-modified anodes and unprepared Pb–Ag alloys were obtained in 0.5 mol L⁻¹ H₂SO₄ electrolyte.

The morphology of the PANI samples was investigated by SEM. The PANI powder was scraped from the substrate, dispersed in potassium bromide, and then compressed into pellets to measure its FTIR spectrum. FTIR spectra were obtained in the KBr phase with a Perkin Elmer (RK-1310) FTIR spectrometer. The surface composition of the PANI-modified anode was determined by XPS (PHI5500, Perkin–Elmer) using Mg K_α X-rays (1253.6 eV) under a pressure of below 5×10⁻⁸ Pa.

3. RESULTS AND DISCUSSION

3.1 Growth processes of PANI film on the Pb–Ag (0.3 wt%) alloy

The formation of a PANI film on the Pb–Ag (0.3 wt%) alloy in aqueous H_2SO_4 solution involves two steps. In the first step, the surface Pb was oxidised [26] and the first nuclei of polyaniline were formed at the same time. The XPS spectra (Figure 11) indicate the lead oxide film is PbO and PbSO_4 film. The PANI film was formed on the PbO film or PbSO_4 film in the second step. Figure 2 shows that the potential of the anode changed during the first 500 s. When the current density was constant at 1.5, 2.5 and 4.5 mA cm^{-2} , the anode potential increased to about 1.7 V and remained steady for about 140 s, then decreased to the final steady potential of about 1.35 V. These changes in the anode potential reflect the PANI growth process. Initially, a defined current density was forced to flow, but electro polymerisation (oxidation) was not sufficient to produce that current. Thus, the potential was shifted to higher values, and formation of PbO_2 may occur. When the potential increased to 1.7 V, above the potential of aniline polymerisation, the PANI granules grew on the Pb–Ag (0.3 wt%) alloy surface. After about 180 s, PANI film covered the alloy surface. The PANI underwent an autocatalytic reaction (mechanism of autocatalytic reaction shown in Figure 1), so the electro polymerisation rate increased. This reaction became sufficiently fast to produce the required current flow, so the potential decreased. Finally, the steady potential (about 1.35 V) was the potential needed to maintain the electro polymerisation reaction at the rate needed to produce the imposed current density.

When the galvanostatic polymerisation current density was 0.5 mA cm^{-2} , the anode potential increased more slowly to about 1.7 V and then decreased more slowly to the steady polymerisation potential of about 1.35 V compared with the potential obtained at the other current densities. Thus, the time needed for the PANI to cover the surface of the sample was longer for PFPbAg-0.5 than for the other current densities.

After 600 s, the potential was stable for all the different polymerisation current densities. Figure 2 shows that a decrease in current density leads to a falling steady potential because it is partially caused by anodic polarisation. The lower the current density is, the lower the polarisation potential is.

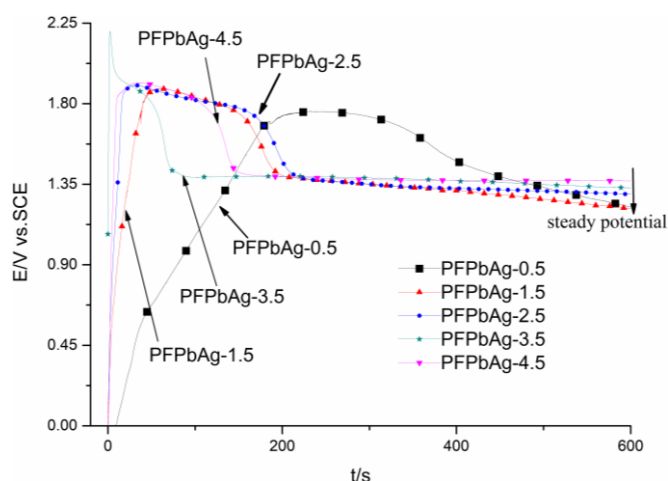


Figure 2. Anode $E - t$ traces for galvanostatic polymerisation of PANI film on Pb–Ag (0.3 wt%) alloy in an aqueous solution containing aniline (0.2 mol L^{-1}) and H_2SO_4 (0.5 mol L^{-1}) at room temperature

3.2 Surface and cross sectional microstructural features for PANI - modified anodes

The SEM images of the surface for the PANI-modified anodes obtained under different galvanostatic polymerisation conditions are shown in Figure 3. The PANI particle size distribution (Figure 4) for the samples was calculated by the software of SEM image analysis Nano Measurer System from the SEM images in Figure 3. The cross-sectional microstructural features for the anode obtained from PFPbAg-3.5 are shown in Figure 5.

Compared with the surface of PANI-modified anodes obtained under low galvanostatic polymerisation current density (as shown in Figure 3 (A, A') and (B, B')) and high galvanostatic polymerisation current density in Figure 3 (D, D'), the morphologies and size of the PANI particles changed as the galvanostatic polymerisation current density changed.

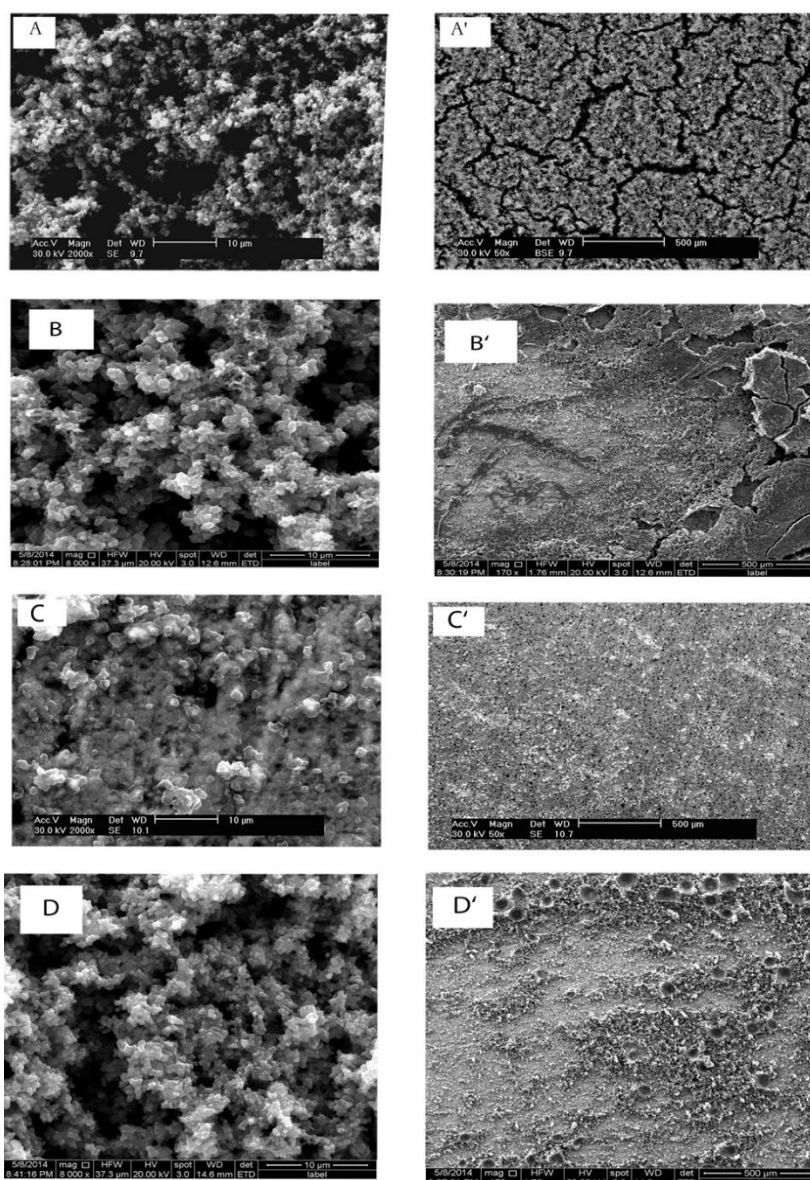


Figure 3. Surface microstructural features of PANI films on Pb–Ag (0.3 wt%) alloy anodes for PFPbAg-0.5 (A,A'), PFPbAg-1.5 (B,B'), PFPbAg-3.5 (C,C') and PFPbAg-4.5 (D,D')

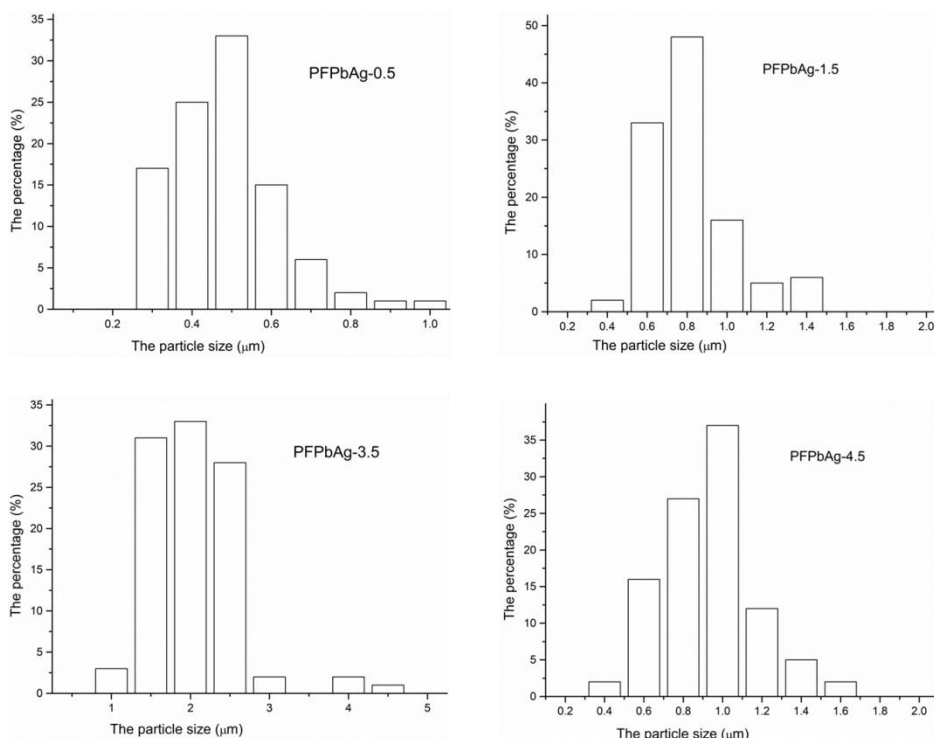


Figure 4. Distributions for PANI particle size of the samples (PFPbAg-0.5, PFPbAg-1.5, PFPbAg-3.5 and PFPbAg-4.5)

According to the results of Figure 4, the particle size distribution was centred at 0.5, 0.8, 2 and 1 μm for PFPbAg-0.5, PFPbAg-1.5, PFPbAg-3.5 and PFPbAg-4.5, respectively. Lower galvanostatic polymerisation current densities (PFPbAg-0.5 and PFPbAg-1.5)) yielded smaller particles. Figure 3 shows cracks in the PANI film for lower current densities, whereas higher current densities (PFPbAg-4.5) yielded structural porosity, and the surface of the PANI film was rough. When the galvanostatic polymerisation current density was 3.5mA cm⁻², the PANI film was densified.

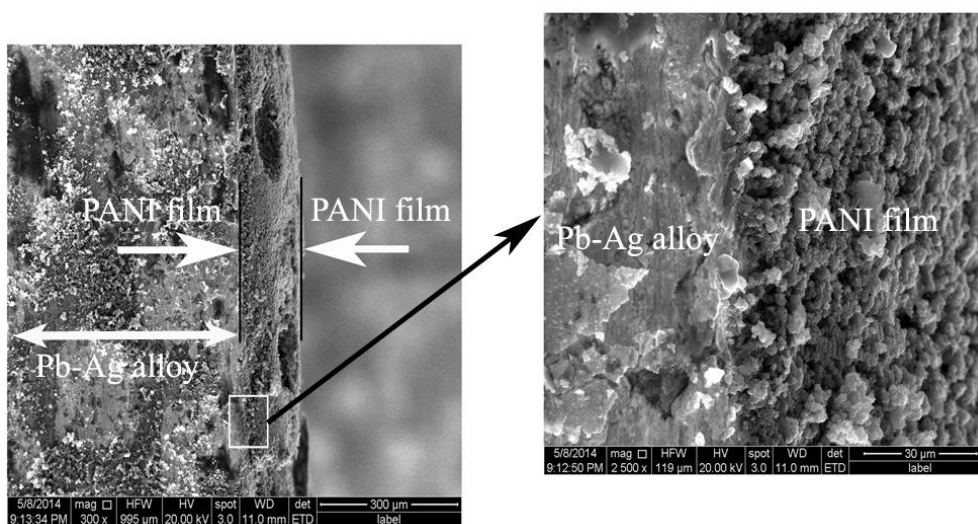


Figure 5. Cross sectional microstructural features of the anode obtained under galvanostatic polymerisation current density 3.5 mA cm⁻².

Figure 5 shows that the thickness of the PANI film was about 140 μm when galvanostatic polymerisation lasted 1200 s, and the growth of the PANI particles expanded from the nuclei.

The growth of three-dimensional hemispherical nuclei was investigated carefully by Scharifker [27], who assumed that the reaction was completely diffusion controlled and obtained the following relationships between the current (I) and the time (t) for nucleation:

For instantaneous nucleation:

$$I = \frac{zFD^2C}{\pi^{\frac{1}{2}}t^{\frac{1}{2}}} [1 - \exp(-N\pi KDt)] \quad (1)$$

For progressive nucleation

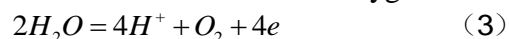
$$I = \frac{zFD^2C}{\pi^{\frac{1}{2}}t^{\frac{1}{2}}} [1 - \exp(-AN_{\infty}\pi KDt^2) / 2] \quad (2)$$

In Equations (1) and (2), zF is the molar charge of the electrodeposited species, D is the diffusion coefficient, c is the bulk concentration, k is a constant, and N is the number of nuclei. The A is nucleation rate per active site, and the N_{∞} is the density of active sites.

Equations (1) and (2) show that the value of A and N_{∞} are important parameters for PANI nucleation on the metal surface during electrosynthesis. Under the same condition, the number of nuclei (N) is equivalent to the same nucleation time (t). Within the same interval Δt , samples with high current will have more charge quantity ΔQ according to the relation $\Delta Q = I\Delta t$. Therefore, lower galvanostatic polymerisation current densities (0.5 and 1.5 mA cm^{-2}) provide minimal charge quantity, the samples yield smaller particles (Figure 3 (A,A') and (B,B')), and the galvanostatic polymerisation current densities (3.5 mA cm^{-2}) yield larger particles, as shown in Figure 3 (C,C'). When the galvanostatic polymerisation current density increased to 4.5 mA cm^{-2} , high current density resulting in polymerisation of aniline grew rapidly. The structure of the PANI film was porous, as shown in Figure 3 (D, D').

3.3 LSV analysis of different anodes

The electrode reaction of oxygen evolution reaction in anode polarisation is:



The equilibrium potential (E_e) of oxygen evolution reaction can be calculated from the Nernst equation according to the parameter of the test condition, and the over-potential of OER is: $\eta = E - E_e$. Therefore, the over potential of the oxygen evolution reaction is determined by OER potential.

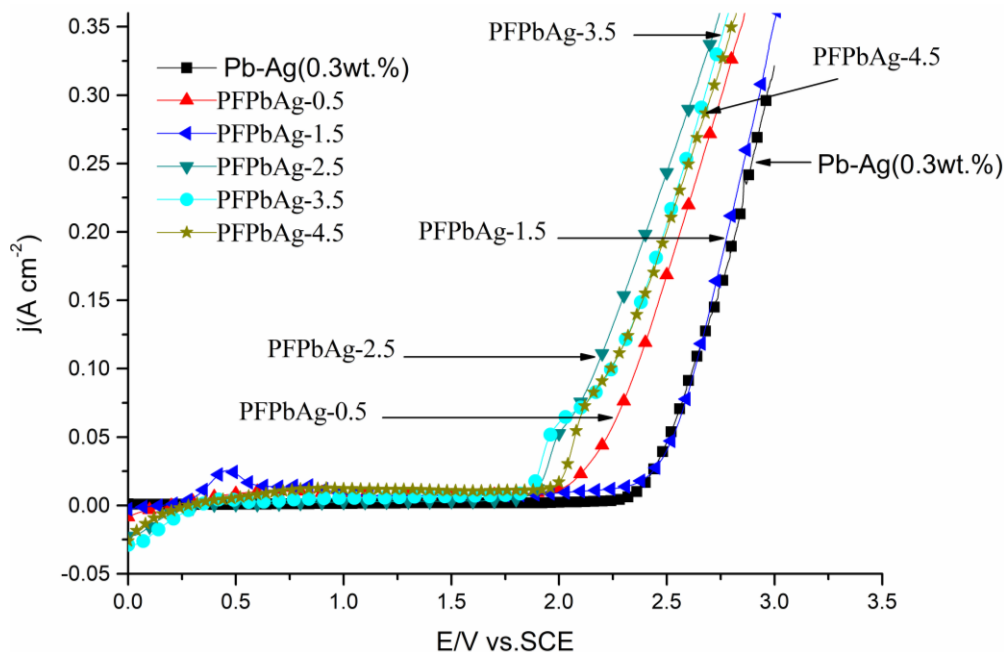


Figure 6. Linear scanning voltammetry curves of the Pb–Ag (0.3 wt%), PFPbAg-0.5, PFPbAg-1.5, PFPbAg-2.5, PFPbAg-3.5 and PFPbAg-4.5 samples at a scanning rate of 1mV/s in 0.5 mol L⁻¹ H₂SO₄ at room temperature.

Figure 6 presents the linear scanning voltammetry of the different PANI-modified anodes. The OER potentials of all PANI-modified anodes are distinctly lower than the potential of unprepared Pb–Ag (0.3 wt%). Figure 6 further shows that PANI-modified anodes had higher anodic current densities at the same anodic potential when the anodic current density was between 25 and 350 mA cm⁻². At the anodic current density between 25 and 75 mA cm⁻² (the typical current density used in industrial zinc electrowinning), PFPbAg-3.5 had the lowest anodic potential, and its minimum OER potential was lower than that of unprepared Pb–Ag (0.3 wt%) by about 500 mV. By contrast, the anodic potential of PFPbAg-2.5 was lowest when the anodic current density was between 75 and 350 mA cm⁻². Furthermore, amongst the modified anodes, the anodic potentials of PFPbAg-0.5 and PFPbAg-1.5 were higher than those of PFPbAg-2.5, PFPbAg-3.5 and PFPbAg-4.5 when the anode started to emit oxygen. The results indicate that the PANI-modified anodes have higher electrocatalysis for the oxygen evolution reaction in aqueous H₂SO₄ electrolyte compared with the unprepared Pb–Ag (0.3 wt%) anode.

3.4 Potentiodynamic polarisation for different anodes

The potentiodynamic polarisation curves in Figure 7 show that the PANI-modified anodes have a lower corrosion current density compared with the unprepared Pb–Ag (0.3 wt%) electrode. The corrosion potentials of all PANI-modified samples are shifted in the positive direction from that of the unprepared Pb–Ag (0.3 wt%) electrode.

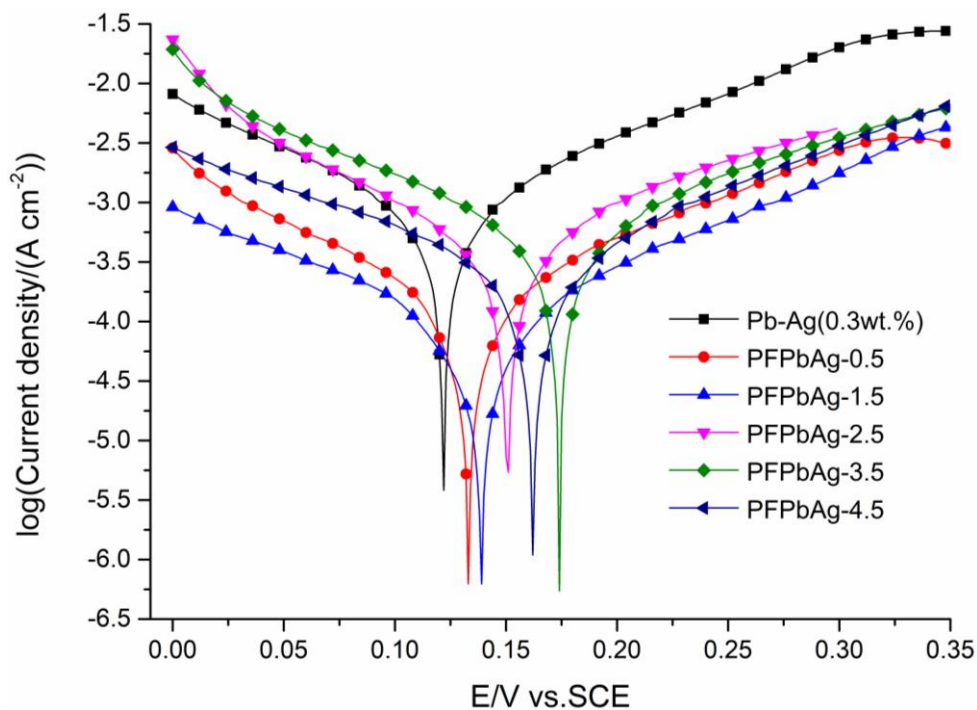


Figure 7. Potentiodynamic polarisation curves of unprepared Pb–Ag (0.3 wt%), PFPbAg-0.5, PFPbAg-1.5, PFPbAg-2.5, PFPbAg-3.5 and PFPbAg-4.5 in $0.5 \text{ mol L}^{-1} \text{ H}_2\text{SO}_4$ at room temperature

3.5 Cyclic voltammetry for the PANI-modified anodes

To evaluate the redox reaction of the PANI modified anodes, the cyclic voltammograms for two typical samples (PFPbAg-0.5 and PFPbAg-3.5) are presented in Figure 8 and 9, respectively.

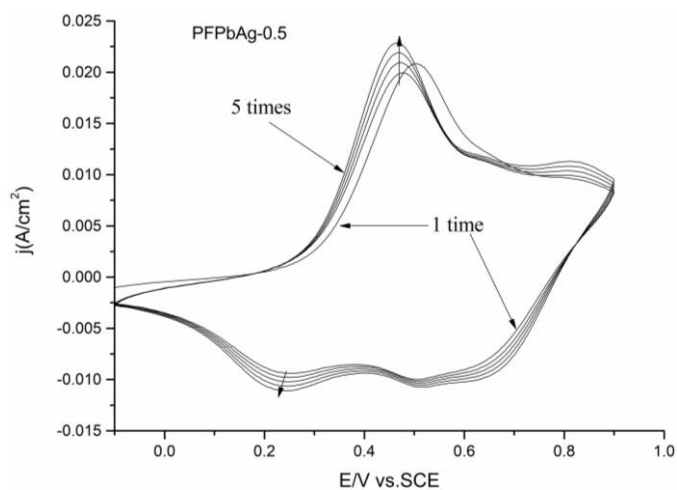


Figure 8. Cyclic voltammograms of PFPbAg-0.5 in $1 \text{ mol L}^{-1} \text{ H}_2\text{SO}_4$ and 0.2 mol L^{-1} aniline, the scan rate was 10 mVs^{-1}

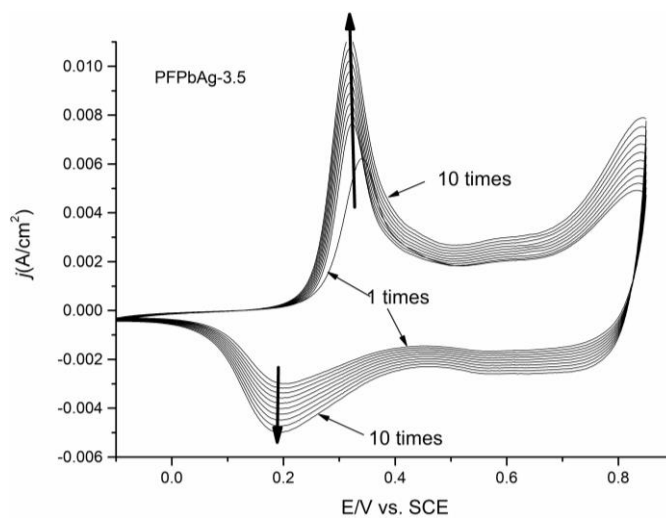


Figure 9. Cyclic voltammograms of PFPbAg-3.5 in 1 mol L^{-1} H_2SO_4 and 0.2 mol L^{-1} aniline, the scan rate was 10 mVs^{-1}

The two samples show clear oxidation and reduction current peaks, which demonstrate that the coating film undergoes a good redox reaction. Martinsa [28] explained that the polyaniline can be interconverted between three different oxidation states, leading to the redox reaction of polyaniline.

The concentration of the protonic acid ions in the electrolyte distinctly influences the electrochemical properties of the PANI [29, 30]. For the cyclic voltammograms of PFPbAg-0.5 in Figure 8, the cyclic voltammograms exhibited two oxidation peaks at about 0.46 and at 0.75 V, but the 0.75 V peak became weaker and exhibited two reduction peaks at about 0.24 and at 0.51 V. However, the cyclic voltammograms of PFPbAg-3.5 in Figure 9 show that the cyclic voltammograms also had two oxidation peaks (0.32 and 0.67 V) and two reduction peaks (0.18 and 0.54 V); the potential of the peaks were lower than that of PFPbAg-0.5.

The anodic current (i_{pa}) and cathodic current (i_{pc}) improved when the current cycles were increased. The reason was that the PANI film became thicker, which enhanced the autocatalytic activity. This phenomenon was reported previously and attributed to autocatalytic PANI film growth [31].

3.6 FTIR spectroscopy

FTIR spectroscopy was employed to investigate the structure of the PANI electropolymerised on the substrate. Figure 10 shows that the FTIR spectrum of the electropolymerised PANI on the modified anode (curve A) is similar to that of the chemical polymerised PANI (curve B).

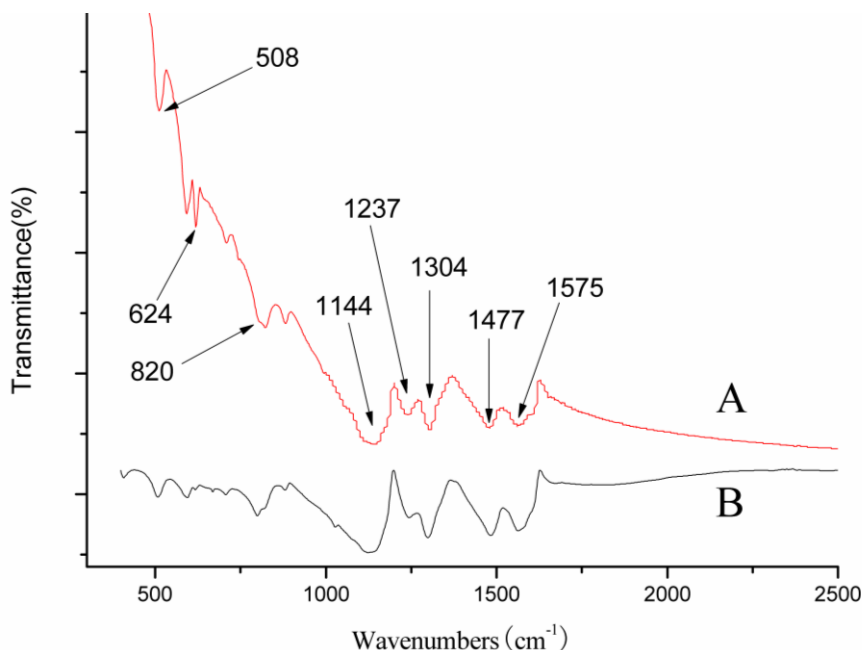
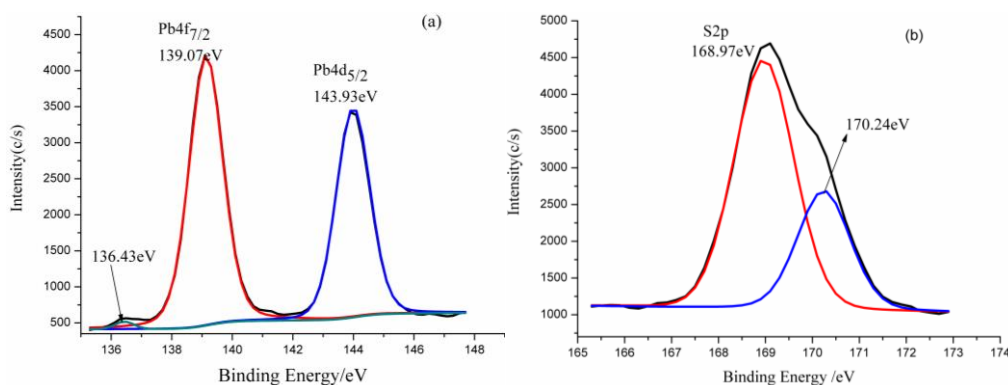


Figure 10. FTIR spectrum of PANI. A: electropolymerised PANI on the modified anode. B: chemical polymerised PANI

The spectrum includes bands corresponding to the emeraldine base forms of PANI at 1659, 1582, 1487, 1274, 1242, 1169, and 827 cm^{-1} [32]. The band at about 1575 cm^{-1} is assigned to quinonoid rings, and the band near 1477 cm^{-1} is attributed to the C–C aromatic ring-stretching vibrations. The absorbance at 1304 cm^{-1} corresponds to the C–N stretching of secondary aromatic amine groups. The absorbance at 1237 cm^{-1} is due to C–N stretching vibrations of aromatic amines, and the peaks at 820 and 1144 cm^{-1} are attributed to bending modes of C–H bonds [24, 33]. In summary, the FTIR spectra confirm that the film on the substrate was PANI.

3.7 X-ray photoelectron spectroscopy

The surface of PFPbAg-3.5 was characterised by XPS to analyse the composition of the surface of the PANI-modified anode.



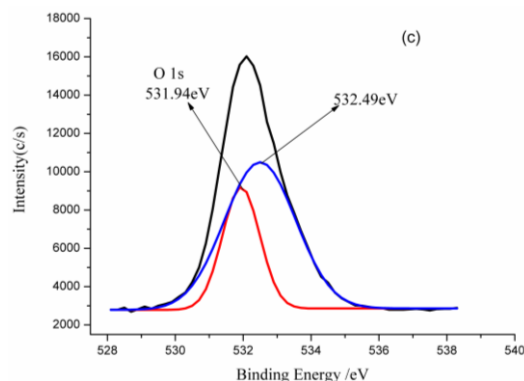


Figure 11. XPS spectra of Pb 4f7/2 and Pb 4f5/2, S2p and O 1s of the surface of the anode obtained under galvanostatic polymerisation current density 3.5 mA cm^{-2} .

The black line in Figure 11a shows the XPS spectra of Pb. The binding energies 136.43, 139.07 (red line in Figure 11a) and 143.93 eV (blue line in Figure 11a) belong to Pb 4f7/2 and Pb 4f5/2. The binding energy values close to that of Pb^{2+} were reported in the literature [34]. The XPS spectra of S2p shown in Figure 11b (black line) can be fitted well with two components. The peaks observed at 168.97 (red line in Figure 11a) and 170.24 eV (blue line in Figure 11a) correspond to SO_4^{2-} reported in the literature [35]. Furthermore, the O1s spectrum shows (Figure 11c) a peak contributed by two components at 531.94 and 532.49 eV. The binding energies values close to SO_4^{2-} are also reported in the literature [35]. In addition, according to Pavlov's work [36], when Pb electrodes are anodised in H_2SO_4 solution, the PbO_n ($1 < n < 2$), PbSO_4 , tet-PbO and PbO_2 species are created on the surface of the anode. Thus, PbSO_4 and PbO films are generated on the surface of the Pb–Ag alloy.

3.8 Discussion

The above research results show that the optimal PANI-modified Pb–Ag alloy anode is the one obtained from galvanostatic polymerisation under the current density of PFPbAg-3.5, and the original electrolyte solution is aniline (0.2 mol L^{-1}) and H_2SO_4 (0.5 mol L^{-1}). It possesses higher electrocatalytic activity and better corrosion resistance in aqueous H_2SO_4 electrolyte; this is related to the properties of PANI film on the anode and the electrochemical active site amounts used for oxidation–reduction transition on the anode surface.

Figure 6 shows that PANI has unique electrocatalysts characteristics in an acidic medium, and the porous structures of PANI film on the substrate provide a larger activity surface than its geometric surface (as shown in Figure 3, 4 and 5), which provides a large area for charge exchange and generates more cation radicals. According to Figure 1, more cation radicals could facilitate the autocatalytic polymerisation of aniline, thereby improving the electrocatalysis of the PANI-modified anodes. Thus, PANI was used as an electrocatalyst or electrocatalyst support materials in the anode. For example, in aqueous H_2SO_4 electrolyte, the polymeric electrodes modified with Pt particles electrodeposited by the programmed potential variation had a better electrocatalytic activity for CO and methanol oxidation [37]. PANI-modified Pt anode provided higher catalysis for HQ/BQ and $\text{Fe}^{2+/3+}$ redox reaction compared with that of Pt anode [38]. Controllable stereoselective synthesis of cis or trans pyrano- and furano-

tetrahydroquinolines was performed via one-pot aza-Diels–Alder reactions catalysed by PANI doped with p-TSA [39]. Our previous work [9] and Xu’s work [40] indicated that PANI has higher electrocatalysis in aqueous H₂SO₄ electrolyte for zinc electrowinning.

The potentiodynamic polarisation curves in Figure 7 show that the corrosion resistance of the PANI-modified anodes are higher than that of the unprepared Pb–Ag (0.3 wt%) electrode. Polyaniline can provide corrosion protection for non-ferrous and ferrous metals substrates [41, 42]. The PANI film coating on the active metals provides corrosion protection through three main mechanisms. Firstly, the PANI film offers a barrier to protect the substrate from the electrolyte [43, 44]. Secondly, Santos [45] reported that the N ion in the amine has an unshared electron pair that can bond to any *d* orbital present on the metal surface. This bonding leads to the formation of a hydrophobic layer that protects the metals.

Thirdly, Kinlen [46] reported that inherently conducting polymer films could protect the metal substrate and maintain an oxide layer on the metal by their redox reaction. At the interface between the PANI film and the Pb–Ag alloy surface, redox reaction takes place. During a complex reaction mechanism, Pb is converted to PbO analogous to the passivation of aluminum to Al₂O₃ [47]. XPS spectra of the surface of PANI-modified anodes are shown in Figure 11. The result indicates the oxidation of Pb.

The protection efficiency (PE) was employed to explicate the corrosion protection of PANI film. The PE was calculated by using the expression [48]:

$$PE\% = \left[\frac{R_{pc} - R_{ps}}{R_{pc}} \right] \times 100\%$$

R_{ps} is the polarisation resistance of the unprepared Pb–Ag (0.3 wt%) electrode, and R_{pc} is the polarisation resistance of the PANI-modified samples. The typical PEs for PFPbAg-2.5 and PFPbAg-3.5 were 93.81 and 83.81%. These results show that the PANI film improved the corrosion protection for the PANI-modified anodes.

In summary, the PANI film that formed on the anodes provides not only a conductive matrix and electrocatalytic activity in the composite inert anodes but also corrosion protection to the substrate. The electrocatalytic activity and corrosion resistance of the PANI-modified anode improve in aqueous H₂SO₄ electrolyte.

4. CONCLUSIONS

A PANI-modified anode consisting of the PANI film coating a Pb–Ag alloy surface is fabricated by performing electro polymerisation. The OER potential of the PANI-modified anode is lower than that of the unprepared Pb–Ag alloy in H₂SO₄ aqueous solution electrolyte. The lowest OER potential is lower than that of unprepared Pb–Ag (0.3 wt%) by about 500 mV. The PANI film acts as a barrier, shares an electron pair with the Pb and undergoes an outstanding redox reaction, so the PANI-modified anodes can exhibit excellent corrosion resistance. Thus, this new anode could improve the electrowinning of nonferrous metals in sulfuric aqueous solution electrolytes. In the future, the stability of the adhesion of the PANI film on the Pb–Ag alloys should be investigated in detail to facilitate real applications of these anodes.

ACKNOWLEDGMENTS

We express our appreciation for the support provided by National Natural Science Funds of China (Grant No. 51004057).

References

1. T. Nguyen, A. Atrens, *J. Appl. Electrochem.*, 38(2008)569.
2. A. Felder, R. Prengaman, *JOM-US*, 58(2006)28.
3. I. Valchanova, Y. Stefanov, K. Stefanov, N. Tabakova, T. Dobrev, *Trans. Inst. Met. Finish.*, 89(2011)210.
4. Z.G. Ye, H.M. Meng, D.B. Sun, *J. Electroanal. Chem.*, 621(2008)49.
5. V.V. Panić, V.M. Jovanović, S.I. Terzić, M.W. Barsoum, V.D. Jović, A.B. Dekanski, *Surf. Coat. Technol.*, 202(2007)319.
6. Z.G. Ye, H.M. Meng, D.B. Sun, *Electrochim. Acta*, 53(2008)5639.
7. J. Aroma, O. Forsén, *Electrochim. Acta*, 51(2006)6104.
8. Y. Li, X.L. Jiang, X.J. Lv, Y.Q. Lai, H.L. Zhang, J. Li, Y.X. Liu, *Hydrometallurgy*, 109(2011)252.
9. H. Huang, J.Y. Zhou, Z.C. Guo, T. Nonferr. Metal. Soc., 20(2010)S55.
10. X.F. Lu, W.J. Zhang, C. Wang, T.C. Wen, Y. Wei, *Prog. Polym. Sci.*, 36(2011)671.
11. A.R. Elkais, M.M. Gvozdenovic, B.Z. Jugovic, J.S. Stevanovic, N.D. Nikolic, B.N. Grgur, *Prog. Org. Coat.*, 71(2011)32.
12. C.G. Granqvist, *Sol. Energy Mater. Sol. Cells*, 91(2007)1529.
13. T.O. Poehler, H.E. Katz, P.C. Searson, *J. Mater. Res.*, 25(2010)1561.
14. R. Silva, T. Asefa, *Adv. Mater.*, 24(2012)1878.
15. Y.T. Shieh, J.J. Jung, R.H. Lin, C.H. Yang, T.L. Wang, *Electrochim. Acta*, 70(2012)331.
16. K.G. Shah, G.S. Akundy, J.O. Iroh, *J. Appl. Polym. Sci.*, 85(2002)1669.
17. P. Zarras, N. Anderson, C. Webber, D.J. Irvin, J.A. Irvin, A. Guenther, J.D. Stenger-Smith, *Radiat. Phys. Chem.*, 68(2003)387.
18. W.A. Marmisollé, M.I. Florit, D. Posadas, *J. Electroanal. Chem.*, 669(2012)42.
19. A. Romeiro, C. Gouveia-Caridade, C.M.A. Brett, *Corros. Sci.*, 53(2011)3970.
20. K.R. Prasad, N. Munichandraiah, *Synth. Met.*, 130(2002)17.
21. G. Wu, K.L. More, C.M. Johnston, P. Zelenay, *Science*, 332(2011)443.
22. A. Zimmermann, U. Künzelmann, L. Dunsch, *Synth. Met.*, 93(1998)17.
23. S.L. Mu, C.X. Chen, J.M. Wang, *Synth. Met.*, 88(1997)249.
24. C.P. Liao, M.Y. Gu, *Thin Solid Films*, 408(2002)37.
25. S.Y. Cui, S.M. Park, *Synth. Met.*, 105(1999) 91.
26. J.L. Camalet, J.C. Lacroix, S. Aeiya, P.C. Lacaze, *J. Electroanal. Chem.*, 445(1998)117.
27. B. Scharifker, G. Hills, *Electrochim. Acta*, 28(1983)879.
28. N.C.T. Martins, T.M.E. Silva, M.F. Montemor, J.C.S. Fernandes, M.G.S. Ferreira, *Electrochim. Acta*, 55(2010)3580.
29. H.N. Dinh, J. Ding, S.J. Xia, V.I. Birss, *J. Electroanal. Chem.*, 459(1998)45.
30. W.S. Huang, B.D. Humphrey, A.G. Macdiarmid, *J. Chem. Soc., Faraday Trans. 1*, 82(1986)2385.
31. R. Greef, M. Kalaji, L. Peter, *Faraday Discuss. Chem. Soc.*, 88(1989)277.
32. N.S. Sariciftci, M. Bartonek, H. Kuzmany, H. Neugebauer, A. Neckel, *Synth. Met.*, 29(1989)193.
33. J. Stejskal, J. Prokeš, M. Trchová, *React. Funct. Polym.*, 68(2008)1355.
34. W.E. Morgan, J.R. Vanwaze, *J. Phys. Chem. Lett.*, 7(1973)964.
35. J.F. Moulder, W.F. Stickle, P.E. Sobol, K.D. Bomben, *Handbook of X-ray Photoelectron Spectroscopy*, Physical Electronics, (1995), Flying Cloud Drive Eden Prairie, Minnesota, USA.
36. D. Pavlov, *Electrochim. Acta*, 23(1978)845.
37. A.M. Castro Luna, *J. Appl. Electrochem.*, 30(2000)1137.

38. Z. Mandić, L. Duić, *J. Electroanal. Chem.*, 403(1996)133.
39. S. Palaniappan, B. Rajender, M. Umashankar, *J. Mol. Catal. A: Chem.*, 352(2012)70.
40. R.D. Xu, L.P. Huang, J.F. Zhou, P. Zhan, Y.Y. Guan, Y. Kong, *Hydrometallurgy*, 22.7(2012)1693.
41. T. Schauer, A. Joos, L. Dulog, C.D. Eisenbach, *Prog. Org. Coat.*, 33(1998)20.
42. M. Rohwerder, A. Michalik, *Electrochim. Acta*, 53(2007)1300.
43. K. Kamaraj, T. Siva, S. Sathiyarayanan, S. Muthukrishnan, G. Venkatachari, *J. Solid State Electrochem.*, 16(2012)465.
44. T. Schauer, A. Joos, L. Dulog, *Prog. Org. Coat.*, 33(1998)20.
45. J.R. Santos, L.H.C. Mattoso, A. Motheo A, *Electrochim. Acta*, 43(1998)309.
46. P.J. Kinlen, D.C. Silverman, C.R. Jefferys, *Synth. Met.*, 85(1997)1327.
47. M.A.S. Oliveira, J.J. Moraes, R. Faez, *Prog. Org. Coat.*, 65(2009)348.
48. P. Pritee, A.B. Gaikwad, P.P.Patil, *Electrochim. Acta*, 52(2007)5958.

© 2019 The Authors. Published by ESG (www.electrochemsci.org). This article is an open access article distributed under the terms and conditions of the Creative Commons Attribution license (<http://creativecommons.org/licenses/by/4.0/>).